Applied Physics Letters ARTICLE scitation.org/journal/apl

Increase of reverse leakage current at homoepitaxial GaN p-n junctions induced by continuous forward current stress

Cite as: Appl. Phys. Lett. **118**, 253501 (2021); doi: 10.1063/5.0053139
Submitted: 5 April 2021 · Accepted: 8 June 2021 ·
Published Online: 22 June 2021

Tetsuo Narita,[1,a)] Yoshitaka Nagasato,[2] Masakazu Kanechika,[3] Takeshi Kondo,[3] Tsutomu Uesugi,[3] Kazuyoshi Tomita,[3] Satoshi Ikeda,[2] Satoshi Yamaguchi,[1] Yasuji Kimoto,[1] Masayoshi Kosaki,[4] Tohru Oka,[4] Jun Kojima,[3] and Jun Suda[3,5]

AFFILIATIONS

[1]Toyota Central R&D Labs., Inc., Nagakute 480-1192, Japan
[2]MIRISE Technologies Corporation, Toyota 470-0309, Japan
[3]Institute of Materials and Systems for Sustainability (IMaSS), Nagoya University, Nagoya 464-8601, Japan
[4]Toyoda Gosei Co., Ltd., Ama, Aichi 490-1207, Japan
[5]Department of Electronics, Graduate School of Engineering, Nagoya University, Nagoya 464-8603, Japan

[a)]**Author to whom correspondence should be addressed:** tetsuo-narita@mosk.tytlabs.co.jp

ABSTRACT

Reliability tests involving the application of high electrical stresses were employed to assess GaN-based vertical p-n junctions fabricated on freestanding GaN substrates with threading dislocation densities less than $10^4\,cm^{-2}$. Electric field crowding at the device edges was eliminated by employing a shallow bevel mesa structure, thus allowing an evaluation of the reliability of the internal p-n junctions. The p-n diodes exhibited reproducible avalanche breakdown characteristics over the temperature range of 25–175 °C. No degradation was observed even during tests in which the devices were held under a reverse bias near the breakdown voltage. Despite this high degree of reliability in response to reverse bias stress, a small number of diodes were degraded during continuous forward current tests, although the majority of diodes remained unchanged. The reverse leakage current exhibited by degraded diodes was increased with an increase in the forward current density within the range of 50–500 A/cm^2, while the breakdown voltages were unchanged in response to current stress. The leakage level increased exponentially with an increase in the total amount of injected carriers but eventually plateaued. In the degraded p-n diode, a luminous point in an emission microscope corresponded to one of the threading dislocations observed in the synchrotron x-ray topography, indicating that a specific dislocation played as a leakage path after injecting carriers.

The realization of sustainable development goals will necessitate the development of clean electrical systems that require minimal energy inputs. Vertical power devices based on gallium nitride (GaN), which has a high breakdown electric field,[1] are expected to be key components in the next-generation electric converters with high blocking voltages and increased current capabilities. As an example, vertical GaN power devices with very low on-state resistances and breakdown voltage values (V_b) of approximately 1 kV have recently been demonstrated.[2–7] A critical requirement related to the practical applications of these devices is that they pass various reliability tests. In high-power electrical systems, such as electric vehicles, such devices can experience either continuous or instantaneous high-voltage stress together with the high-density current stress and elevated junction temperatures. In the case of silicon carbide (SiC), carrier injection into a p-n junction will expand Shockley-type stacking faults present at basal plane dislocations in a process referred to as bipolar degradation. This can lead to current leakage in a reverse-biased junction as well as increased on-state resistance.[8,9] Bipolar degradation can also be harmful to unipolar metal–oxide–semiconductor field-effect transistors (MOSFETs) if the body diodes are forward-biased during the switching operation, and this issue has limited the practical applications of SiC-based power devices for some time now. The reliability of GaN, when subjected to high-density current stress, has also been a concern with regard to applications involving laser diodes (LDs) and

high-power light-emitting diodes (LEDs). Specifically, current injection in LDs can result in the degradation of the threshold current[10–12] and monotonic increases in the reverse bias leakage current.[11] Increases in the forward and reverse leakage currents in response to high current stress have also been reported to occur in high-power LEDs.[13,14] The appearance of a reverse leakage current can additionally be a significant concern in vertical GaN power devices, although the current density in such devices is typically much lower than the values in LDs.

To date, there has been only limited research concerning the reliability of vertical GaN power devices, because 1 kV class units have been launched over the last several years. In addition, there are various technical issues that have prevented the evaluation of the reliability of these devices. The initial failures of GaN-on-GaN p-n diodes likely occur on the surface as a consequence of electric field crowding and so do not reflect the intrinsic properties of the material.[15,16] The surface morphologies of these units will also affect their reverse bias characteristics. As an example, growth pits originating from particles can reduce the V_b values of p-n diodes.[17] Rough surface structures, such as hillocks or macrosteps, can also increase the reverse leakage current[18] and/or result in non-uniform avalanche breakdown due to fluctuations in the incorporation of carbon.[19,20] These failures related to the device geometry and surface morphology should be eliminated so that they do not affect the results of reliability tests.

The present work assessed the reliability of internal p-n junctions within GaN-on-GaN diodes having double-side-depleted shallow bevel terminations[1] that completely eliminated surface electric field crowding. These p-n diodes, which were free of both pits and macrosteps, were evaluated while applying reverse bias stress up to the avalanche voltage at temperatures from 25 to 175 °C and under the stress of high-density current injection. Despite their apparent high degree of stability under reverse bias stress, a small number of GaN-based p-n diodes demonstrated a critical failure mode induced by the continuous forward current test.

Non-punch-through p-n junctions were grown via metalorganic vapor phase epitaxy (MOVPE) on 51 mm-diameter freestanding GaN substrates, employing an acidic ammonothermal method. The threading dislocation (TD) density of these substrates was typically in the range of 10^3–10^4 cm^{-2}. Analyses by secondary ion mass spectrometry showed that the MOVPE procedure generated, going from top to bottom, a 0.1 μm-thick p^+ contact layer doped with magnesium (Mg) at 5×10^{19} cm^{-3}, a 1.5 μm-thick p-type GaN layer with a Mg concentration of 5.3×10^{17} cm^{-3}, a 1.5 μm-thick n-type GaN layer doped with silicon (Si) at 3.2×10^{17} cm^{-3}, and a 0.2 μm-thick n^+ layer with a Si concentration of 1.1×10^{18} cm^{-3}. A shallow beveled mesa was formed on each test device using a combination of thermal reflow (in conjunction with a thick photoresist) and subsequent chloride-based inductively coupled plasma reactive ion etching to a depth of 2.6 μm.[1] The mesa angle of each circular device, having a 443 μm diameter at the junction, was typically 6.2°. A Ni/Au anode electrode with a 320 μm diameter was formed on each p^+GaN contact layer by electron beam deposition and was subsequently sintered at 500 °C under gaseous oxygen. Finally, a Ti/Al/Ni metal stack was deposited on the backside of the substrate as a cathode electrode. The cross-sectional schematic of the fabricated diodes can be seen in Fig. S1 in the supplementary material.

Assuming a relative permittivity of 10.4 for GaN,[21] we estimated the effective doping concentration for these devices based on the results of capacitance–voltage measurements. This value was calculated as $N_aN_d/(N_a + N_d)$, where N_a and N_d are the donor and acceptor concentrations, respectively, and a value of 1.4×10^{17} cm^{-3} was obtained. Based on our previous research concerning the impact ionization coefficients and $N_aN_d/(N_a + N_d)$ values for GaN,[22] the present devices were anticipated to have a critical breakdown field value of 3.26 MV/cm and a V_b of 219 V at room temperature. Figure 1 presents forward and reverse current–voltage (I–V) curves obtained from three representative diodes (referred to as #1DX, #2DX, and #3DX) and demonstrates that all diodes generated essentially the same curves. The diodes were assessed for threading dislocations by the synchrotron-radiation x-ray topographical analysis at the SPring-8 facility after the measurements of initial forward and reverse I–V characteristics (i.e., before the series of stress tests as described later), using a previously reported method.[23] Diodes #1DX and #2DX were found to contain at least five and four threading dislocations, respectively, while diode #3DX had no observable dislocations. The number of threading dislocations was possibly underestimated in the synchrotron x-ray topography analyses in the case that a TD contrast involved more than one TD. Figures 1(b)–1(d) also demonstrate peaks related to transient increases in leakage current during a low reverse bias sweep for each sample, possibly due to the discharge of carriers from deep traps.[24] The experimental V_b values were within the range of 212–215 V at 25 °C, indicating that the degree of electric field crowding at the mesa surfaces in these specimens was negligibly small. Our previous simulations[25] have shown that electric field crowding can be completely eliminated using a [Mg]/[Si] ratio of 1.65 and a mesa angle

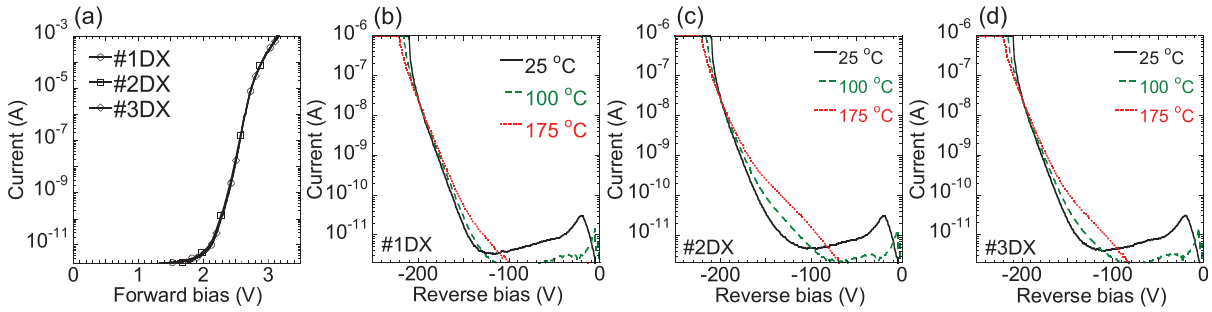

FIG. 1. (a) Forward I–V curves obtained from all three representative diodes at 25 °C and [(b)–(d)] reverse I–V curves for these same diodes acquired over the temperature range of 25–175 °C. The junction and anode electrode in these devices had sizes of 443 and 320 μm, respectively.

of 6.2°. The breakdown characteristics of these devices were found to be reproducible, and the V_b values were slightly increased with an increase in temperature, indicating avalanche breakdown. Observations by Nomarski microscopy after forming the beveled mesa structures confirmed that all three units had pit-free and macrostep-free morphologies. Thus, the reliability of internal p-n junctions could be assessed without any effect of failures related to external geometry or morphology.

The reverse bias characteristics of each device did not change after ten sweeps up to 169 V (80% of V_b) at 25, 100, and 175 °C [see Figs. S2(a)–S2(c) in the supplementary material]. The reverse leakage currents were also constant when the specimens were held under a reverse bias of 169 V for 1 h at these temperatures [see Figs. S2(d)–S2(f) in the supplementary material]. Subsequently, the highest stress reverse bias tests were performed based on holding the devices at 1 mA for 1 h at 25, 100, and 175 °C, in which the devices were kept in the avalanche state. As shown in Fig. 2, the reverse voltages showed little change throughout the test periods. This indicates both the avalanche robustness of these diodes and the intrinsic durability of GaN-based p-n junctions under a reverse bias. These characteristics would provide an advantage with regard to the fail-safe operation of GaN-based vertical power devices.

We subsequently performed continuous current injection tests. In these experiments, the current density, J, was increased in a stepwise manner in conjunction with a forward bias, applying values of 50, 100, 200, and 500 A/cm^2 for a time span of 1 h each. Note that, here, J is normalized by the area of the anode electrode. Current stress was accumulated during these tests, and the forward and reverse characteristics of each device were monitored at regular intervals. Figures 3(a)–3(c) present the forward I–V curves acquired before and after these continuous J stress tests, and confirm that the forward characteristics were unchanged throughout each trial. Increases in the on-state resistance and turn-on voltage values, such as associated with the bipolar degradation of SiC-based p-n junctions, were not observed in these GaN-based devices. However, the diode #2DX did exhibit a drastic increase in reverse leakage current in response to the high J stress, as shown in Fig. 3(e), indicating an irreversible degradation. In contrast, the reverse I–V curves for diodes #1DX and #3DX were unchanged [Figs. 3(d) and 3(f)]. Table I summarizes the results obtained from this series of reliability tests for the three diodes. Similar continuous current injection tests were performed using a total of twelve diodes, including the present three diodes, although the seven diodes not shown in the present paper were designed to have V_b values of 247–248 V, and the different J stresses up to 2000 A/cm^2 were applied. Four of these diodes showed increases in reverse leakage current during the continuous J stress tests, while the other eight diodes were not degraded. These results suggest that the failure of the reverse bias characteristics in response to a high J stress would be expected to occur in a small proportion of such diodes. It should also be noted that this type of failure would be more significant in the case of a device having a larger area with a high current capability.

We characterized the failure of the reverse characteristics induced by the high J stress. As shown in Fig. 4(a), the reverse leakage current at 100 V tended to increase exponentially with the increase in the total quantity of injected carriers but eventually plateaued. Figure 4(b) demonstrates that the leakage current obtained from the diode #2DX after the injection tests exhibited a weak correlation with temperature, with an apparent activation energy of approximately 52 meV. The conduction mechanism associated with this phenomenon requires further investigation. There have been some reports of increases in reverse leakage current in the case of LDs, LEDs, and p-n diodes subjected to high current stress,[11,13,14,20,26] although the forward bias characteristics of these devices were also degraded. This degradation of the forward bias characteristics of LDs involved increases in the threshold current density, as well as the series resistance and recombination-generation current at a low forward bias. These effects have been attributed to the diffusion of point defects, which are proportional to the square root of the stress time.[11,12,26] In contrast, in the present study, we did not observe any degradation of the forward bias characteristics. In addition, the exponential increase in the reverse leakage current as a function of the quantity of injected carriers and the eventual plateau cannot be explained based on point defect diffusion. One possible interpretation for the results shown in Fig. 4(a) is that the carrier injection produced a conductive effect that promoted local current leakage. Once sufficient carrier injection had occurred to produce this conductive state, the leakage current plateaued. The unchanged V_b values in Fig. 3(e) suggest that the majority of the p-n junction functioned properly even after degradation, meaning that the reverse leakage induced by the high J stress was due to local degradation.

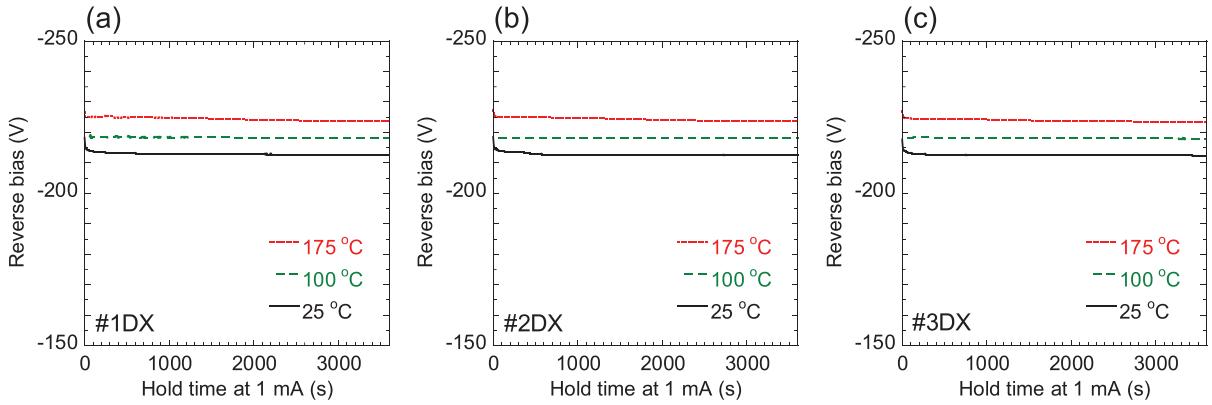

FIG. 2. Reverse bias as a function of stress time at a constant current of 1 mA and in the avalanche state for diodes (a) #1DX, (b) #2DX, and (c) #3DX.

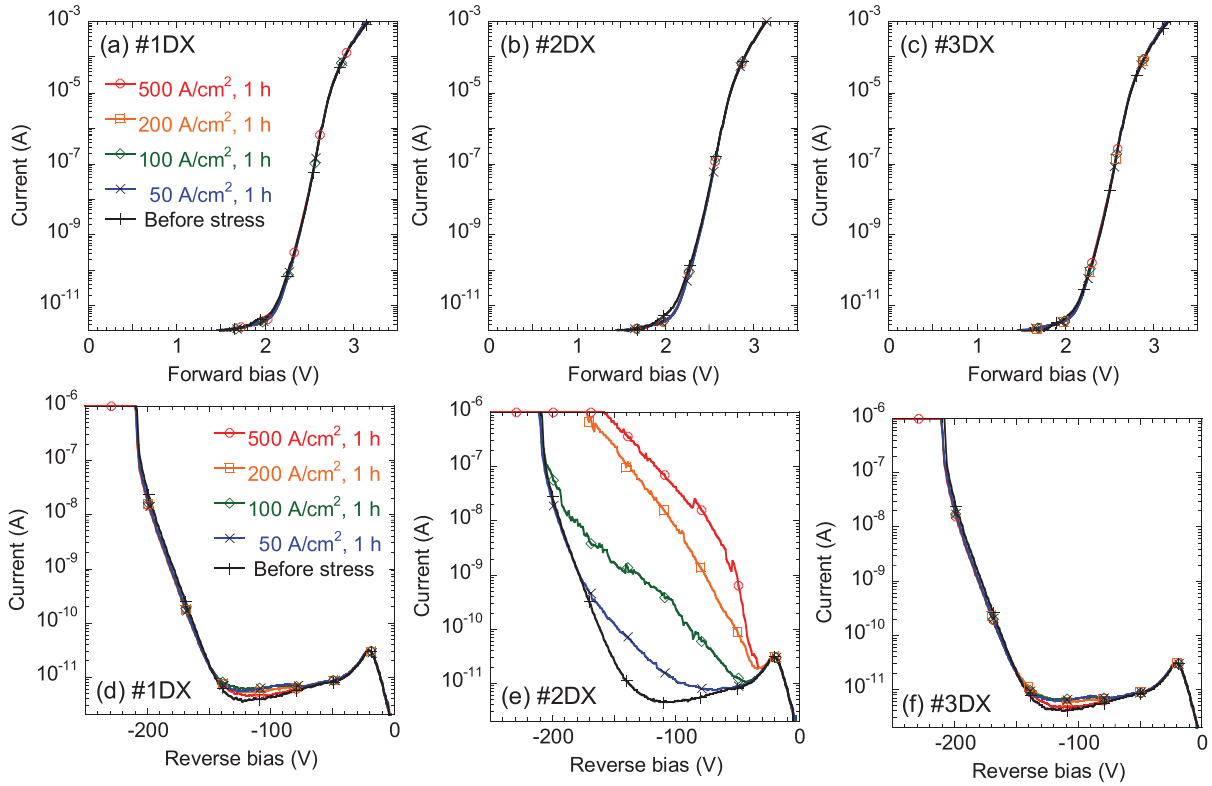

FIG. 3. Forward *I–V* curves obtained from diodes (a) #1DX, (b) #2DX, and (c) #3DX before and after current injections at $J = 50$, 100, 200, and 500 A/cm^2 for 1 h (where J is normalized by the anode electrode area). Bottom panels show reverse *I–V* curves before and after the respective J stresses for 1 h for diodes (d) #1DX, (e) #2DX, and (f) #3DX.

To identify the current leakage path, we performed the emission microscopy (EMS) observation for the degraded diode #2DX. The EMS measurement is an effective technique to identify the leakage spots when defects, such as TDs, provide the reverse leakage paths, resulting in carrier recombination.[27] The detectable wavelength range was 900 to 1600 nm, and the positional accuracy of an emission spot was around 1 μm. For a reverse bias of more than 100 V, the leakage current above 100 nA is detectable as an emission spot on an empirical basis. Since carriers were mostly injected under the anode electrode during the continuous J stress tests, the EMS observation was performed from the backside of substrate after removing the backside electrode via polishing. Figure 5 shows the synchrotron x-ray topography and EMS images at the reverse bias of 129 V for the diode #2DX. There were at least four threading dislocations having white contrasts in the synchrotron x-ray topography image in Fig. 5(a). The luminous point in the EMS image corresponded to one of the threading dislocations as seen in the arrow of Fig. 5(b), while the other three dislocations exhibited no emission. This suggests the leakage after J stress was the result of specific threading dislocations. Indeed, the diode #3DX (which had no obvious dislocations) showed no degradation in response to a high J stress (Table I). However, the diode #1DX, having at least five dislocations, remained unchanged throughout the high J stress test, suggesting that the majority of dislocations in this device did not contribute to the degradation. In the case of SiC, a Shockley-type staking fault is a cause of bipolar degradation phenomena and is expanded by carrier injection,[8,9] whereas line defects, such as

TABLE I. Summary of the sequential reliability tests applied to representative diodes. The tests were performed in the order from left to right shown here. The number of threading dislocations (TDs) was estimated by the synchrotron x-ray topography analyses before the series of stress tests. V_r and I_r show stress conditions of a reverse voltage and a reverse current.

Diode	Number of TDs	10 sweeps $V_r = 0$ to -169 V at 25, 100, 175 °C	1 h hold $V_r = -169$ V at 25, 100, 175 °C	1 h hold $I_r = 1$ mA at 25, 100, 175 °C	Forward J stress 50, 100, 200, 500 A/cm^2 at 25 °C
#1DX	5	Passed	Passed	Passed	No degradation
#2DX	4	Passed	Passed	Passed	Increased reverse current
#3DX	0	Passed	Passed	Passed	No degradation

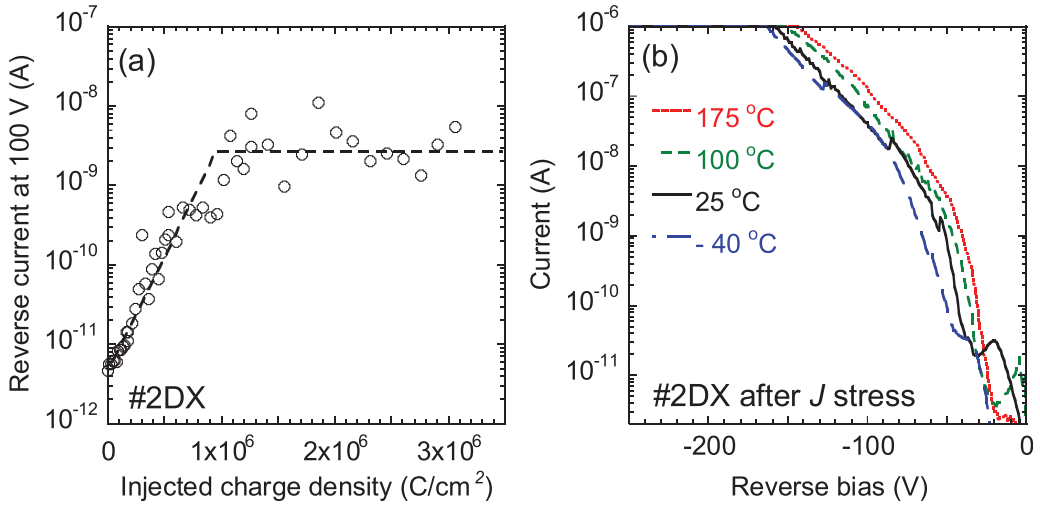

FIG. 4. (a) Reverse leakage current at 100 V as a function of the total amount of injected carriers per anode electrode area for the diode #2DX at 25 °C and (b) temperature-dependent reverse *I–V* curves obtained after the current injection tests for the diode #2DX.

threading edge dislocations, are harmless. On the contrary, the increase in the reverse leakage in the GaN p-n diode occurred at a specific threading dislocation based on Fig. 5. If the dislocations were expanded by carrier injection, the luminous point in the EMS would not agree with the threading dislocation observed before the continuous *J* stress test. Therefore, the degradation mode in the present study would have a completely different mechanism from the bipolar degradation in SiC p-n junctions. Although the electrical properties of threading dislocations have been studied,[24,28–33] the irreversible changes that can occur in response to electrical stress have not yet been clarified. Thus, identifying the origin of the present degradation will require further investigation to characterize defects in degraded and degradation-free diodes.

In conclusion, we applied various reliability tests to GaN-on-GaN p-n junctions while eliminating external factors, such as electric field crowding and morphology issues. No degradation was seen following ten reverse bias sweeps and a 1 h hold test at a reverse bias equal to 80% of V_b over the temperature range of 25–175 °C.

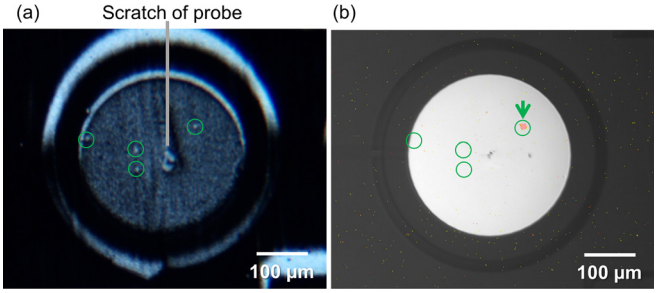

FIG. 5. (a) Synchrotron x-ray topography image for the diode #2DX, and (b) the EMS image for the corresponding diode after continuous *J* stress test. The circles show the threading dislocations which had white contrasts in the x-ray topography image. The EMS observation was performed from the backside under the current of 300 nA at 129 V. A luminous point in the EMS was observed in one of the threading dislocations [indicated by an arrow in (b)].

Furthermore, 1 mA hold tests in association with a reverse bias in the avalanche state induced only minimal changes in *I–V* characteristics. Despite the apparent high stability of these devices under a reverse bias, current injection tests under forward biases increased the reverse leakage current for a small number of diodes. The reverse leakage current was found to increase exponentially with an increase in the total amount of injected carriers and eventually plateaued. This degradation mode could impact the reliability of junction FETs in which carriers are injected from gates and also affect the switching operation of unipolar MOSFETs in which the body diodes are forward biased.

See the supplementary material for the schematic image of the fabricated p-n diode having a shallow bevel mesa termination (Fig. S1), the reverse current–voltage (*I–V*) characteristics during ten sweeps up to 169 V at each temperature of 25, 100, and 175 °C [Figs. S2(a)–S2(c)], and the reverse leakage current under a reverse bias of 169 V for 1 h at these temperatures [Figs. S2(d)–S2(f)].

The authors thank the Center for Integrated Research of Future Electronics, Transformative Electronics Facilities (C-TEFs) at Nagoya University for fabricating the devices used in this work. The synchrotron radiation x-ray topography analyses were performed at the BL16B2 (Proposal Nos. 2018B5370, 2019A5370, 2019B5370, and 2020A5370) and BL20B2 (Proposal Nos. 2019B1042 and 2020A1039) beamlines at the SPring-8 facility with the approval of the Japan Synchrotron Radiation Research Institute (JASRI).

DATA AVAILABILITY

The data that support the findings of this study are available from the corresponding author upon reasonable request.

REFERENCES

[1]T. Maeda, T. Narita, H. Ueda, M. Kanechika, T. Uesugi, T. Kachi, T. Kimoto, M. Horita, and J. Suda, in *IEEE International Electron Devices Meeting* (IEEE, San Francisco, 2018), p. 687.

[2]H. Nie, Q. Diduck, B. Alvarez, A. P. Edwards, B. M. Kayes, M. Zhang, G. Ye, T. Prunty, D. Bour, and I. C. Kizilyalli, IEEE Electron Device Lett. **35**, 939 (2014).
[3]T. Oka, T. Ina, Y. Ueno, and J. Nishii, Appl. Phys. Express **8**, 054101 (2015).
[4]D. Shibata, R. Kajitani, M. Ogawa, K. Tanaka, S. Tamura, T. Hatsuda, M. Ishida, and T. Ueda, in *IEEE International Electron Devices Meeting* (IEEE, San Francisco, 2016), p. 248.
[5]Y. Zhang, M. Sun, D. Piedra, J. Hu, Z. Liu, Y. Lin, X. Gao, K. Shepard, and T. Palacios, in *IEEE International Electron Devices Meeting* (IEEE, San Francisco, 2017), p. 215.
[6]R. Tanaka, S. Takashima, K. Ueno, H. Matsuyama, and M. Edo, Jpn. J. Appl. Phys., Part 1 **59**, SGGD02 (2020).
[7]J. Liu, M. Xiao, Y. Zhang, S. Pidaparthi, H. Cui, A. Edwards, L. Baubutr, W. Meier, C. Coles, and C. Drowley, in *IEEE International Electron Devices Meeting* (IEEE, Virtual, 2020), p. 477.
[8]T. Kimoto, Jpn. J. Appl. Phys., Part 1 **54**, 040103 (2015).
[9]H. Tsuchida, K. Murata, T. Tawara, M. Miyazato, T. Miyazawa, and K. Maeda, in *IEEE International Electron Devices Meeting* (IEEE, San Francisco, 2019), p. 470.
[10]L. Marona, P. Wisniewski, P. Prystawko, I. Grzegory, T. Suski, S. Porowski, P. Perlin, R. Czernecki, and M. Leszczyński, Appl. Phys. Lett. **88**, 201111 (2006).
[11]M. Meneghini, N. Trivellin, K. Orita, S. Takigawa, T. Tanaka, D. Ueda, G. Meneghesso, and E. Zanoni, Appl. Phys. Lett. **97**, 263501 (2010).
[12]P. Perlin and Ł. Marona, "InGaN laser diode degradation," in *Materials and Reliability Handbook for Semiconductor Optical and Electron Devices*, edited by O. Ueda and J. Pearton (Springer Science+Business Media, New York, 2013), Chap. 8, pp. 247–261.
[13]M. Meneghini, A. Tazzoli, G. Mura, G. Meneghesso, and E. Zanoni, IEEE Trans. Electron Devices **57**, 108 (2010).
[14]L. Liu, M. Ling, J. Yang, W. Xiong, W. Jia, and G. Wang, J. Appl. Phys. **111**, 093110 (2012).
[15]K. Nomoto, B. Song, Z. Hu, M. Zhu, M. Qi, N. Kaneda, T. Mishima, T. Nakamura, D. Jena, and H. G. Xing, IEEE Electron Device Lett. **37**, 161 (2016).
[16]B. Rackauskasa, M. J. Uren, T. Kachi, and M. Kuball, Microelectron. Reliab. **95**, 48 (2019).
[17]F. Horikiri, Y. Narita, T. Yoshida, H. Ohta, T. Mishima, and T. Nakamura, in *International Conference on Compound Semiconductor Manufacturing Technology* (CS MANTECH, Miami, 2016), p. 275.
[18]I. C. Kizilyalli, P. Bui-Quang, D. Disney, H. Bhatia, and O. Aktas, Microelectron. Reliab. **55**, 1654 (2015).
[19]H. Fujikura, K. Hayashi, F. Horikiri, Y. Narita, T. Konno, T. Yoshida, H. Ohta, and T. Mishima, Appl. Phys. Express **11**, 045502 (2018).
[20]H. Fukushima, S. Usami, M. Ogura, Y. Ando, A. Tanaka, M. Deki, M. Kushimoto, S. Nitta, Y. Honda, and H. Amano, Jpn. J. Appl. Phys., Part 1 **58**, SCCD25 (2019).
[21]A. S. Barker, Jr. and M. Ilegems, Phys. Rev. B **7**, 743 (1973).
[22]T. Maeda, T. Narita, S. Yamada, T. Kachi, T. Kimoto, M. Horita, and J. Suda, in *IEEE International Electron Devices Meeting* (IEEE, San Francisco, 2019), p. 70.
[23]M. Kanechika, S. Yamaguchi, M. Imanishi, and Y. Mori, Jpn. J. Appl. Phys., Part 1 **58**, SCCD22 (2019).
[24]B. Rackauskas, S. Dalcanale, M. J. Uren, T. Kachi, and M. Kuball, Appl. Phys. Lett. **112**, 233501 (2018).
[25]T. Maeda, T. Narita, H. Ueda, M. Kanechika, T. Uesugi, T. Kachi, T. Kimoto, M. Horita, and J. Suda, IEEE Electron Device Lett. **40**, 941 (2019).
[26]E. Fabris, M. Meneghini, C. De Santi, Z. Hu, W. Li, K. Nomoto, X. Gao, D. Jena, H. G. Xing, G. Meneghesso, and E. Zanoni, Microelectron. Reliab **88–90**, 568 (2018).
[27]M. Meneghini, N. Trivellin, M. Pavesi, M. Manfredi, U. Zehnder, B. Hahn, G. Meneghesso, and E. Zanoni, Appl. Phys. Lett. **95**, 173507 (2009).
[28]T. Kachi and T. Uesugi, Sens. Mater. **25**(3), 219–227 (2013).
[29]T. Nakano, M. Araidai, K. Shiraishi, A. Tanaka, Y. Honda, and H. Amano, ECS Trans. **86**, 41 (2018).
[30]S. Usami, Y. Ando, A. Tanaka, K. Nagamatsu, M. Deki, M. Kushimoto, S. Nitta, Y. Honda, H. Amano, Y. Sugawara, Y.-Z. Yao, and Y. Ishikawa, Appl. Phys. Lett. **112**, 182106 (2018).
[31]S. Usami, N. Mayama, K. Toda, A. Tanaka, M. Deki, S. Nitta, Y. Honda, and H. Amano, Appl. Phys. Lett. **114**, 232105 (2019).
[32]T. Nakano, Y. Harashima, K. Chokawa, K. Shiraishi, A. Oshiyama, Y. Kangawa, S. Usami, N. Mayama, K. Toda, A. Tanaka, Y. Honda, and H. Amano, Appl. Phys. Lett. **117**, 012105 (2020).
[33]T. Narita and T. Kachi, "Future challenges: Defects in GaN power devices due to fabrication processes," in *Characterization of Defects and Deep Levels for GaN Power Devices*, edited by T. Narita and T. Kachi (AIP Publishing, Melville, NY, 2020), Chap. 8, pp. 8-1–8-6